The Journal of Experimental Biology 212, 639-647
Published by The Company of Biologists 2009
doi:10.1242/jeb.022798

Plasma membrane calcium ATPase required for semicircular canal formation and otolith growth in the zebrafish inner ear

Shelly Cruz[1], Jen-Chieh Shiao[2,*], Bo-Kai Liao[1], Chang-Jen Huang[3,4] and Pung-Pung Hwang[1,4,*]

[1]Institute of Fisheries Science, College of Life Science, National Taiwan University, Taipei, Taiwan, [2]Institute of Oceanography, College of Science, National Taiwan University, Taipei, Taiwan, [3]Institute of Biological Chemistry, Academia Sinica, Nankang, Taipei, Taiwan and [4]Institute of Cellular and Organismic Biology, Academia Sinica, Nankang, Taipei, Taiwan

*Authors for correspondence (e-mails: jcshiao@ntu.edu.tw; pphwang@gate.sinica.edu.tw)

Accepted 24 November 2008

SUMMARY

Fish otoliths consist of >90% calcium carbonate, the accretion of which depends on acellular endolymph. This study confirms the presence of plasma membrane calcium ATPase 1a isoform (Atp2b1a) in the auditory and vestibular system of a teleost fish. As shown by *in situ* hybridization, zebrafish *atp2b1a* is expressed mainly in larval otic placode and lateral-line neuromast as well as in the hair cells within the adult zebrafish inner ear chamber. Zebrafish *atp2b1a* knockdown by antisense morpholinos reduced the number of hair cells and produced malformation of semicircular canals and smaller otoliths. These defects coincide with unbalanced body orientation. The formation of smaller otoliths in *atp2b1a* morphants may stem from an impairment of calcium supply in the endolymph. However, otolith formation persists in most morphants, suggesting that other zebrafish Atp2b isoforms or paracellular pathways may also transport calcium into the endolymph. These results suggest that Atp2b1a plays an important role for normal development of the auditory and vestibular system as well as calcium transport in the inner ear of zebrafish.

Supplementary material available online at http://jeb.biologists.org/cgi/content/full/212/5/639/DC1

Key words: labyrinth, auditory system, deafness, vestibule, calcium transport, otolith.

INTRODUCTION

The inner ear functions as an auditory and vestibular system in vertebrates. The cochlea, the hearing organ in birds and mammals, is absent in the inner ear of the teleost. Otic chambers, which contain otoconia or accreting otoliths and three semicircular canals are shared features between teleosts and other vertebrates (Popper and Fay, 1997). Otoliths of fish and otoconia of other vertebrates function as mechanoreceptors. The inner ear is stimulated by differential movement between the dense otolith and less dense sensory epithelium, which causes bending of hair bundles on the epithelium. This stimulation allows the inner ear to detect sound and motion (Popper and Lu, 2000).

Some key proteins are known to be involved in defining the morphological and molecular basis of the sensory organ in the inner ear (Bryant et al., 2002). For instance, an active calcium transporter known as plasma membrane calcium ATPase isoform 2 (ATP2B2) is of physiological importance in the development of the inner ear in mammals (Kozel et al., 1998). ATP2B2 was suggested to be the major isoform in the mammalian inner ear based on high and restricted expression in several cell types, such as cochlear out hair cells and spiral ganglion cells (Kozel et al., 1998). Thus ATP2B2 is considered to be of specialized physiological importance in auditory systems compared to other isoforms (Furuta et al., 1998). In addition, Stauffer et al. (Stauffer et al., 1995) showed that ATP2B1 and four isoforms in mammals are the house-keeping genes, responsible for cellular homeostasis. However, little is known about the physiological role of Atp2b2 and other isoforms in the development of teleost inner ear (Shull, 2000).

Teleost sagittal otoliths are mostly composed of the aragonite form of calcium carbonate. A composition of 99.8% $CaCO_3$ in the otolith of adult trout (Borelli et al., 2001) illustrates the high involvement of calcium for otolith daily growth. Driven by thermodynamic controls, aqueous calcium (Ca^{2+}) and carbonate ions (CO_3^{2-}) in the endolymphatic fluid bind together to form calcium carbonate, which is deposited on the otolith (Romanek and Gauldie, 1996). Proteins extracted from tilapia (*Oreochromis niloticus*) otolith chambers reveal high calcium-binding capacity, which promotes otolith calcification (Sasagawa and Mugiya, 1996).

Otoliths grow continually throughout the life of a fish (Campana and Neilson, 1985), but the otoconia size in other vertebrates is fixed after the individual matures. This suggests a higher and ongoing requirement for calcium transport to the inner ear of fish in comparison to mammals. Based on the study of calcium transport by Mugiya and Yoshida (Mugiya and Yoshida, 1995), cytosolic calcium is extruded to the apical side of saccular cells proximal to the otolith by active intracellular pathways. Using mannitol, a marker for paracellular ion traffic, Mugiya and Yoshida (Mugiya and Yoshida, 1995) suggested that intercellular junctions were too tight to allow the marker to penetrate into the endolymph, thus negating the possibility of a paracellular pathway. Conversely, Payan et al. (Payan et al., 2002) revealed a linear endolymph $^{45}Ca^{2+}$ gradient by perfusion proximal to the saccular epithelium in trout, suggesting passive diffusion through a paracellular pathway. In addition, Ibsch et al. (Ibsch et al., 2004) found pronounced calcium precipitates at the proximal surface of the otolith between the sensory epithelium and the otolith, and suggested that calcium incorporation takes place in this region. A paracellular calcium pathway was also suggested based on the observation of calcium precipitates at macular junctions (Ibsch et al., 2004). These contradictory findings were based on kinetic, pharmacological and histological techniques. To date, there

are no molecular, biochemical or cellular data to support any of these calcium transport models for the inner ear of fish.

It is believed that active and transcellular calcium transport in fish gills is mediated by the epithelial calcium channel at the apical side and a plasma membrane calcium ATPase (PMCA) and/or a sodium–calcium exchangers (NCX) at the basolateral side (Hwang and Lee, 2007). However, the role of active calcium transport in the teleost inner ear is largely unknown. Six PMCA isoforms and seven NCX isoforms of zebrafish were identified in our recent study (Liao et al., 2007) and only one PMCA isoform (*atp2b1a*) was expressed in the inner ear of larval zebrafish (Liao et al., 2007). This observation indicated that Atp2b1a isoform might be involved in the development of the zebrafish inner ear. In the present study, the role of Atp2b1a isoform was elucidated in zebrafish in order to clarify the role of calcium transport in teleost inner ear development.

Abundant bioinformation and genetic tools are available for zebrafish, facilitating the study of inner ear development in this species. The optical clarity of larval zebrafish enables the direct observation of otic defects induced by experimental manipulations during the early stages of development (Whitfield et al., 2002). Increasing knowledge of otolith formation and inner ear development in fish may enhance our understanding of diseases and disorders affecting hearing and balance in other vertebrates, including humans.

MATERIALS AND METHODS

The experimental animal

Zebrafish (*Danio rerio* Hamilton 1822, AB strain) adults were obtained from laboratory stock. All fish handling complied with the protocol "Animal care and utilization of Academia Sinica" for experiments on animals. Fish were maintained at a density of three to six individuals per liter of water at 26–29°C. We generally followed the method described by Shiao et al. (Shiao et al., 2005) to dissect and obtain adult inner ear tissue. Inner ear total RNA was extracted from 30–50 adults with TRIZOL reagent (Invitrogen, Carlsbad, CA, USA), following the standard protocol, and was used for cDNA synthesis using the Invitrogen Superscript III (SSIII) kit.

RNA probe synthesis

The full-length *atp2b1a* cDNA was obtained by PCR (forward 5′-GGCTAACAACTCATACAGCGGGG-3′ and reverse 5′-GGC-GTGGTCAATTTCATCAAGGT-3′) amplification and inserted into the pGEM-T easy vector (Promega, Madison, WI, USA) for the synthesis of antisense and sense RNA probes. Purified plasmids were then linearized by restriction enzyme digestion, and *in vitro* transcription was performed with T7 and SP6 RNA polymerase (Roche, Penzberg, Germany), respectively, in the presence of digoxigenin (dig)-UTP. Dig-labeled RNA probes were examined with RNA gels and dot-blot assays to confirm quality and concentration. For dot-blot assays, synthesized probes and standard RNA probes were spotted on nitrocellulose membrane according to the manufacturer's instructions. After cross-linking and blocking, the membrane was incubated with an alkaline phosphatase-conjugated anti-dig antibody and stained with nitro blue tetrazolium (NBT) and 5-bromo-4-chloro-3-indolyl phosphate (BCIP).

In situ hybridization

In situ hybridization was performed on whole larvae and on the lagenar chamber of adult zebrafish as previously described (Pan et al., 2005). Fish were anesthetized with buffered MS-222 before dissection and fixation. Zebrafish embryos of each stage and lagenar chambers dissected from adult zebrafish were fixed with 4% paraformaldehyde overnight, and then washed several times with phosphate-buffered saline (PBS). Fixed samples were rinsed with PBST (0.2% Tween 20, 1.4 mmol l^{-1} NaCl, 0.2 mmol l^{-1} KCl, 0.1 mmol l^{-1} Na_2HPO_4, 0.002 mmol l^{-1} KH_2PO_4; pH 7.4), and incubated with hybridization buffer (HyB) containing 60% formamide, 5×SSC, and 0.1% Tween 20 for 5 min at 65°C. Prehybridization was performed in HyB^+, which is the hybridization buffer supplemented with 500 μg ml^{-1} yeast tRNA and 25 μg ml^{-1} heparin for 2 h at 65°C. After prehybridization, samples were incubated in 100 ng of the RNA probe in 300 μl of HyB^+ at 65°C overnight for hybridization. Samples were then washed at 65°C for 10 min in 75% HyB and 25% 2×SSC, 10 min in 50% HyB and 50% 2×SSC, 10 min in 25% HyB and 75% 2×SSC, 10 min in 2×SSC, and twice for 30 min in 0.2×SSC at 70°C. Further washes were performed at room temperature for 5 min in 75% 0.2×SSC and 25% PBST, 5 min in 50% 0.2×SSC and 50% PBST, 5 min in 25% 0.2×SSC and 75% PBST, and 5 min in PBST. After serial washings, samples were incubated in blocking solution containing 2% sheep serum and 2 mg ml^{-1} BSA in PBST for 2 h and then incubated in 1:10,000 alkaline phosphatase-conjugated anti-dig antibody in blocking solution at 4°C overnight. After incubation, samples were washed with PBST and transferred to the staining buffer. The staining reaction was held with NBT and BCIP in staining buffer until the signal was sufficiently strong. The staining reaction was terminated by several washings in DEPC-PBST. Then the samples were fixed with 4% paraformaldehyde for 20 min and washed twice with PBST for 5 min each before storage at 4°C in a dark box.

Zebrafish *atp2b1a* knockdown by morpholino oligonucleotide

An antisense morpholino oligonucleotide (MO) 5′-GCTGT-ATGAGTTGTTAGCCATGTC-3′ (nucleotides –3 to 22) was designed by Gene Tools (Philomath, OR, USA) and directed against the *atp2b1a* start codon to block protein translation. The same morpholino with five nucleotides changed (mismatched MO) was used for the control group (5′-GgTGaATGAcTTGTTAGCgAT-cTC-3′). To obtain a large morphant sample size, we injected the MO (resuspended in 1× Danieau buffer: 58 mmol l^{-1} NaCl, 0.7 mmol l^{-1} KCl, 0.4 mmol l^{-1} $MgSO_4$, 0.6 mmol l^{-1} $Ca(NO_3)_2$, 5 mmol l^{-1} Hepes, pH 7.6) into embryos at the one- to four-cell stage. Dosage of 6 ng was found (range: 2–12 ng) to be the most efficient and caused less non-specific abnormality in preliminary experiments. All the embryos were incubated under the constant temperature of 29°C.

To further confirm the specificity of antisense MO, we inserted the *atp2b1a* partial sequence spanning the target site of antisense MO sequence into a pCS2 vector with a green fluorescent protein (GFP) construct. The pCS2_*atp2b1a*:GFP was sequenced to confirm the construct. Using the construct, synthesized capped mRNAs (cRNAs) by SP6 mMessage mMachine kit (Ambion, Austin, TX, USA) were generated. Capped mRNAs at 300 pg per embryo were co-injected with or without the antisense MO (6 ng) at one- to two-cell stages. Then, the embryos were incubated at 29°C for further observations.

Morphological development, including otolith and semicircular canal formation, was observed from the first 24 h up to 7 days post-fertilization (dpf) using a stereomicroscope (Olympus SZX 12, Tokyo, Japan) and a compound light microscope (Zeiss Axioplan 2, Oberkochen, Germany). Photographs of the sagittal otoliths of 80 morphants (injected with 6 or 12 ng MO) and 40 wild-type fish were taken at 2–7 dpf. The maximal diameters of sagittal otoliths were measured using the software Image-Pro plus (Media

Cybernetics 1994, Silver Spring, MD, USA). If the *atp2b1a* morphants had fused otoliths, the sagittae and lapilli still could be identified and the maximal diameters of sagittal otoliths were measured from the otolith edge that was not connected to the lapilli. To investigate the behavior of *atp2b1a* morphants, zebrafish embryos were injected with 6, 3 and 2 ng MO and the fish were observed under the stereomicroscope at 6 dpf. The *atp2b1a* morphants that could not maintain their balance either at rest or while moving were considered balance-defective individuals and both abnormal and normal fish were counted.

Staining of hair cells, hair bundles and ionocytes

Zebrafish embryos at different stages were anesthetized with buffered MS-222 and the fish fixed in 4% paraformaldehyde in 0.1 mol l^{-1} phosphate buffer (PB; pH 7.4) for approximately 1–4 h at 4°C. Fixation was followed by washing in PBS several times, then by treatment with 2% Triton X-100 (Sigma) for 1 h at room temperature and washed again in PBS. Fish were immersed in 3% bovine serum albumin (BSA) at room temperature for 30 min to block nonspecific binding, followed by incubation in primary antibody in PBS for 1–2 nights at 4°C. Monoclonal antibody HCS-1 (1:100) was kindly provided by J. T. Corwin (Finley et al., 1997). HCS-1 can specifically label the cell bodies of hair cells in the inner ear of zebrafish (Blasiole et al., 2006). Samples were washed in PBS twice for 10 min and incubated with PBS-diluted secondary antibody goat anti-mouse IgG conjugated with FITC (1:300; Jackson Immunoresearch Laboratories, West Grove, PA, USA) for 2 h at room temperature. After washing, FITC-conjugated phalloidin solution (30 nmol l^{-1}) was used to label the hair bundle of the hair cells for 10–30 min at room temperature.

DASPEI [2-(4-dimethylaminostyryl)-*N*-ethylpyridinium iodide], a mitochondrial vital probe, was used to stain the hair cells in the neuromasts (Harris et al., 2003) and epidermal ionocytes (Hiroi et al., 1999), which are mitochondria-rich cells. Live samples of both morphants and wild-type fish were immersed in tap water with DASPEI (100 ppm) for 30 min in a dark box.

Samples stained with fluorescent dyes were immediately examined under a confocal laser scanning microscope (TCS-NT, Leica Lasertechnik, Heidelberg, Germany).

Measurement of whole-body calcium contents and influx

Whole-body calcium content and influx were measured following the method of Chen et al. (Chen et al., 2003) with a minor modification. Calcium content of *atp2b1a* morphants (injected with 6 ng MO) and of wild-type fish were measured at 2, 4 and 6 dpf using an atomic absorption spectrophotometer (Hitachi Z-5000, Tokyo, Japan). Each analysis contained ten replicates and each replicate had five larvae. Larvae were anesthetized with MS-222 and digested in 13.1 mol l^{-1} HNO_3 at 60°C. Digested solutions were diluted with double-deionized water and then measured using the atomic absorption spectrophotometer. Standard solutions from Merck (Darmstadt, Germany) were used to make standard curves.

Morphants (injected with 6 ng antisense MO) and the wild-type zebrafish (five replicates, three larvae each) at 2, 4 and 6 dpf were incubated in tap water containing 4 ml $^{45}Ca^{2+}$ for 4 h. After incubation, samples were washed with isotope-free tap water three times and anesthetized with MS-222 before digestion. Samples were digested with tissue solubilizer (Solvable, Packard, Meriden, CT, USA) in the counting vial at 50°C overnight. After digestion, 1 ml counting solution was added (Ultima Gold, Packard) and the radioactivity counted with a liquid scintillation β-counter (LS6500, Beckman, Fullerton, CA, USA). The calcium influx rate was calculated by the following formula:

$$J_{in} = Q_{embryo}\, X_{out}^{-1}\, t^{-1}\, W^{-1}\,, \quad (1)$$

where J_{in} is the influx rate (pmol mg^{-1} h^{-1}), Q_{embryo} is the radioactivity of the embryo (c.p.m. per individual) at the end of incubation, X_{out} is the specific activity of the incubation medium (c.p.m. pmol^{-1}), t is the incubation time (h), and W (mg) is the wet body mass, estimated from 50 pooled larvae at each developmental stage.

Statistical analysis

Values are presented as the mean ± standard deviation (s.d.). One-way analysis of variance (ANOVA) was used to evaluate sagittal otolith growth, calcium content and calcium influx between wild-type zebrafish and *atp2b1a* morphants. Differences among groups were identified by Tukey's pairwise multiple comparison test. The Mann–Whitney rank sum test was used to evaluate the number of hair cells in the neuromast and in the inner ear between wild-type zebrafish and *atp2b1a* morphants. Significance was set at $\alpha<0.05$.

RESULTS

Gene cloning and expression of *atp2b1a* in zebrafish

Searching the zebrafish genome database in NCBI and Ensembl enabled us to identify a human ATP2B homolog in zebrafish. Specific primers were designed according to the sequence, and full-length cDNA of the zebrafish *atp2b1a* was cloned and sequenced. The DNA sequence was submitted to GenBank with the accession no. DQ242508. The cloned gene is a full-length cDNA with a 284 bp 5′UTR and a 151 bp 3′UTR, and the coding region is 3648 bp (including the stop codon), which encodes a 1215 deduced amino

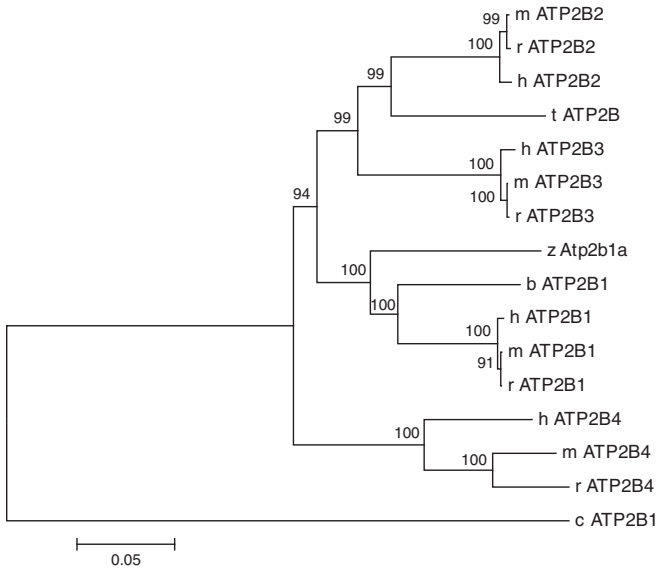

Fig. 1. Phylogenic analysis of ATP2B amino acid sequences. The consensus tree was constructed using the neighbor-joining method with bootstrap of 1000 times and poisson correction (Mega-3 software). Bootstrap values are shown at the branches. The GenBank accession numbers of the sequences used are as follows: P20020 (h ATP2B1), Q01814 (h ATP2B2), Q16720 (h ATP2B3), P23634 (h ATP2B4), P11505 (r ATP2B1), P11506 (r ATP2B2), Q64568 (r ATP2B3), Q64542 (r ATP2B4), NP_080758 (m ATP2B1), NP_033853 (m ATP2B2), NP_796210 (m ATP2B3), NP_998781 (m ATP2B4), AAK11272 (b ATP2B1bx), AAK15034 (t ATP2B), AAR00672 (c ATP2B); b, bullfrog; c, *C. elegans*; h, human; m, mouse; r, rat; t, tilapia; z, zebrafish. The bar represents 5% replacement of amino acids per site.

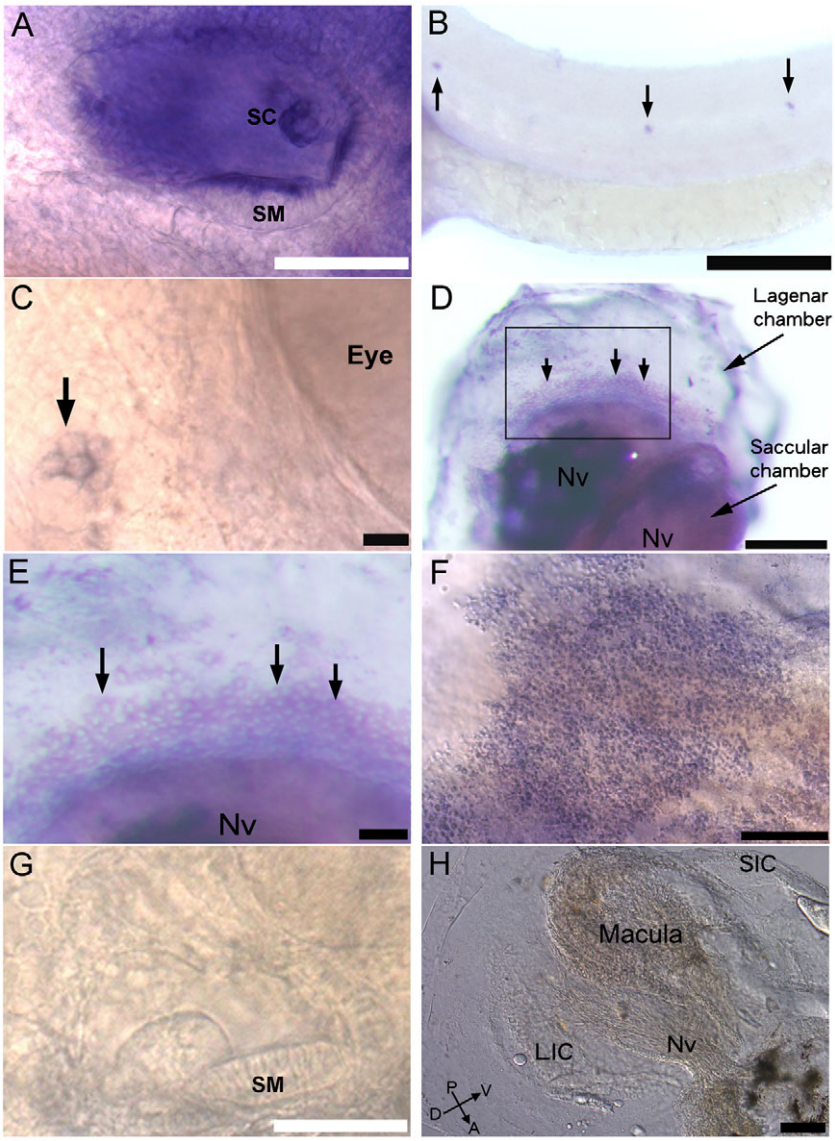

Fig. 2. Zebrafish *atp2b1a* mRNA expression pattern revealed by *in situ* hybridization. (A–C) Zebrafish *atp2b1a* mRNA is localized in the inner ear (A) and lateral-line neuromasts (indicated by arrows in B,C). The larval inner ear (2 dpf) shows ubiquitous staining with prominent staining in the hair cells of sensory macula (SM), the sensory crista and the protrusion of the semicircular canals (SC). (D,E) Basolateral view of the lagenar chamber of an adult fish with the otolith inside the chamber. *atp2b1a* expression was detected in numerous cells around the sensory macula as indicated by the arrows in D. (E) Higher magnification of the boxed area in D. (F) Apical view of the lagenar chamber showing the strong staining of *atp2b1a* in the hair cells in the macula. (G,H) The sense probe, as a control, does not reveal signals in the inner ear of the larvae (G) or the lagenar chamber of the adult (H). A, anterior; D, dorsal; LIC, lagenar ionocytes; Nv, hearing nerve; P, posterior; SIC, saccular ionocytes; V, ventral. Scale bars, 200 μm (B), 100 μm (A,D,F,G,H), 20 μm (E), 10 μm (C).

acid sequence. A phylogenetic tree of ATP2b amino acid sequence was generated using the neighbor-joining analysis (Mega version 3.1) (Kumar et al., 2004) (Fig. 1). The analysis included the entire amino acid sequence of zebrafish (z Atp2b1a), human (h ATP2B), mouse (m ATP2B), rat (r ATP2B), bullfrog (b ATP2B), tilapia (t ATP2B) and *Caenorhabditis elegans* (c ATP2B). The ATP2Bs were roughly clustered into four groups with isoforms from each species forming a clustered group 1–4. *C. elegans* ATP2B was not classified into any vertebrate ATP2B isoform and constituted a unique lineage. According to the phylogenetic analysis, zebrafish Atp2b1a belongs to the ATP2B1 isoform family (Fig. 1). This nomenclature was approved by the Zebrafish Nomenclature Committee (http://zfin.org/zf_info/nomen.html#Approval). Zebrafish Atp2b1a shares high identities (70–80%) with ATP2B of mammals, bullfrogs (AAK11272) and tilapia (AAK15034) and relatively lower identities (49%) with invertebrate ATP2B (*C. elegans*: AAR00672).

Whole-mount *in situ* hybridization confirmed ubiquitous expression of *atp2b1a* in the inner ear with high concentrations in the sensory macula and sensory crista. These high concentrations were accompanied by visible outgrowths of the semicircular canal in zebrafish larvae at 2 dpf (Fig. 2A). The expression of *atp2b1a* in the semicircular canals was also observed in larval zebrafish at 4 and 5 dpf. This result indicated that atp2b1a may play an important role in the development of semicircular canals. In addition, *atp2b1a* was also localized in the neuromasts of the lateral line system of zebrafish larvae (Fig. 2B,C). The expression of *atp2b1a* mRNA can be detected in these tissues by *in situ* hybridization from 1–5 dpf embryos. The expression of *atp2b1a* mRNA was also found in some cells in the periphery of the sensory macula in adult otolith chambers (Fig. 2D,E). Judging from the cellular morphology and the location, these cells could be ionocytes or transition cells, which usually appeared in several rows at the periphery of the sensory macula (Shiao et al., 2005). *atp2b1a* mRNA was also traced to the hair cells of the otolith chamber in adult zebrafish. The staining of numerous hair cells was observed from the apical view of the otolith chamber after removing the otolith to expose the sensory macula as shown in Fig. 2F. Zebrafish *atp2b1a* sense probe was used as a control and did not reveal any signals either in the larval or adult inner ear (Fig. 2G,H). By browsing the Ensembl Genome database (zebrafish assembly version 6, searched with the SSAHA2 algorithm), zebrafish *atp2b1a* is linked to the genome locus on chromosome 4 at location 17,525,704–17,571,442 bp, where an annotated PMCA, *si:dkey-18o7.1* (Ensembl gene ID: ENSDARG00000012684) was found. The *si:dkey-18o7.1* is a temporary name derived from the zebrafish

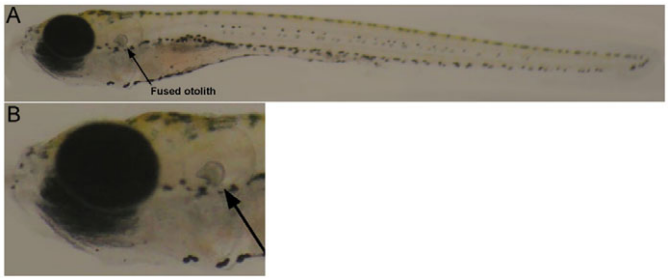

Fig. 3. Zebrafish *atp2b1a* morphant at 5 dpf shows normal body morphology (A) and abnormal inner ear with the fused otolith (B, indicated by the arrow).

genome sequencing and annotation project of the ZFIN database and its expression pattern is available on the ZFIN web site (http://zfin.org/cgi-bin/webdriver?MIval=aa-markerview.apg&OID=ZDB-GENE-030925-29). The gene *si:dkey-18o7.1* was specifically expressed in several tissues, including, otic vesicle, lateral line system, brain and olfactory placode. These expression patterns were consistent with our data.

Phenotypes of *atp2b1a* knockdown by antisense morpholino oligonucleotides

Blocking the protein translation of *atp2b1a* by antisense morpholino oligos (MO) resulted in the disruption of inner ear development, and did not cause other evident defects as observed from the morphology (Fig. 3). Embryos were injected with 6, 3 and 2 ng of *atp2b1a* MO and were observed at 6 dpf. Fish with 72%, 18% and 10% of each treatment could not maintain their balance either at rest or while moving (N=150 for each treatment). This dose-dependent response of behavioral phenotypes suggested that the injection of MO was within a reasonable range. Mismatched MO injection did not cause abnormal behavior of the fish.

Knockdown of *atp2b1a* resulted in decreased otolith accretion, abnormal otolith number (Fig. 4D,F), failure of otoliths to grow at proper locations (Fig. 4C,E,F), and the aberrant protrusion of semicircular canals (Fig. 4D,E,F). Mismatched MO injection had no apparent effect on development in the inner ear, as treated fish were similar to the wild-type fish, as shown in Fig. 4G.

Some morphants showed no otolith formation. For most morphants, otoliths were formed but the seeding of the otolith precursors occurred several hours later than in wild-type larvae. *atp2b1* morphants with only one otolith were frequently observed and this may be due to the seeding failure of the otolith precursor (Fig. 4A,B). The precursors of lapilli and sagittae may have seeded in the wrong location resulting in decreased distance between the two structures (Fig. 4C). As the lapilli and sagittae accreted, the two otoliths would eventually connect and fuse to become a single otolith. The fused otoliths were observed as early as 30 hpf although most fused otoliths occurred around 40–48 hpf.

Normally degradation of the injected capped mRNAs starts at 2 dpf as observed with decreased GFP signal in embryos with injected capped mRNA alone, therefore, data could be only gathered between 1–2 dpf. In the capped mRNA-GFP group the green fluorescence

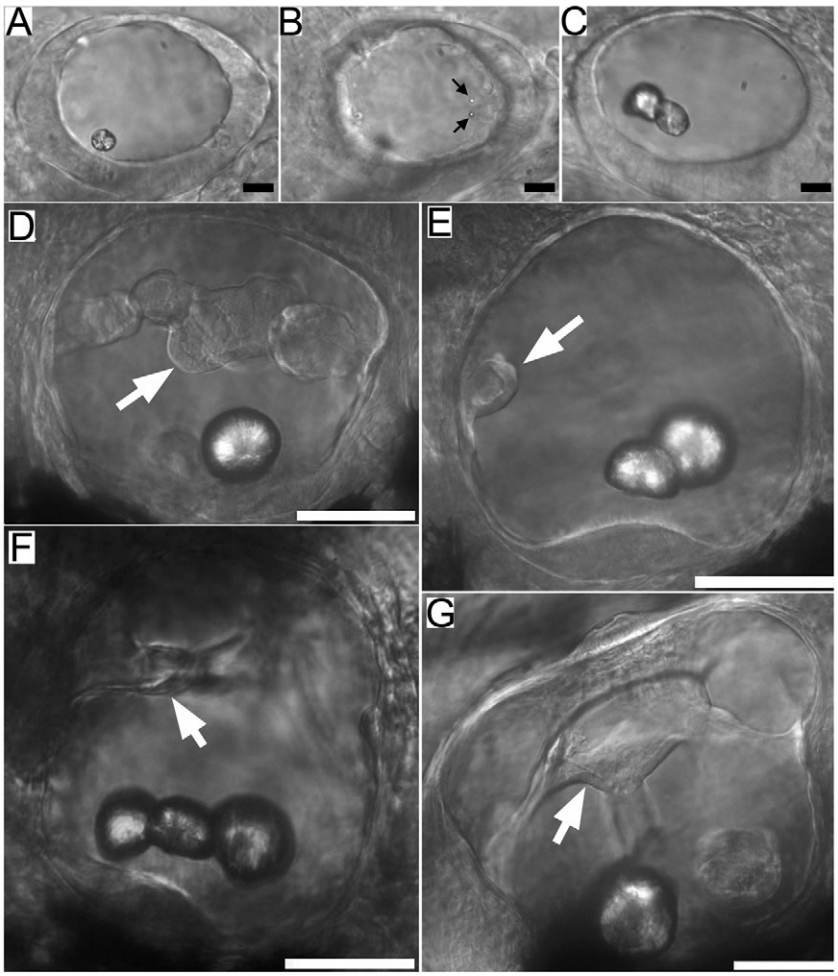

Fig. 4. Zebrafish inner ear phenotypes of wild-type and morphants with anterior to the left in all panels. (A,B) Different focal planes of the same placode of a zebrafish *atp2b1a* morphant at 35 hpf. A shows a normal lapillus has formed but the sagitta failed to crystallize. B shows two otolith precursor particles, indicated by the black arrows. (C) Another zebrafish *atp2b1a* morphant (35 hpf) showing the fused otoliths, with the sagitta wrongly located in the anterior area of the placode. (D–F) Zebrafish *atp2b1a* morphants (4 dpf) with one, two or three fused otoliths and disrupted or reduced outgrowth of semicircular canals. (G) Wild-type larva (4 dpf) with two otoliths and normal outgrowth of the semicircular canals in the inner ear. Semicircular canals are indicated by the white arrows. Scale bars, 10 μm (A–C); 50 μm (D–G).

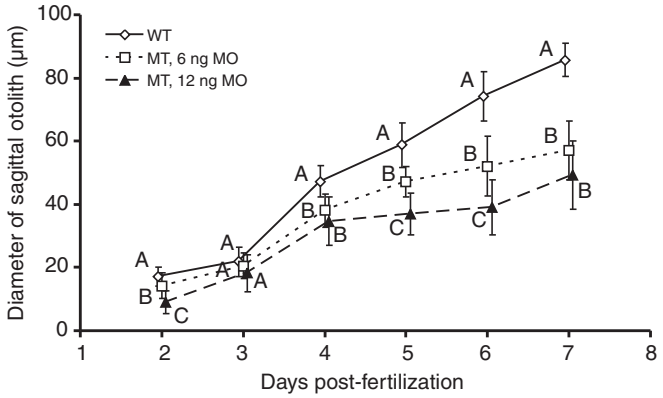

Fig. 5. Comparison of sagittal otolith accretion in *atp2b1a* morphants (MT) and wild-type (WT) zebrafish. Otoliths of *atp2b1* morphants were significantly smaller than those of the wild-type larvae. Higher doses of antisense morpholinos (MO) result in smaller otoliths. A, B and C indicate significant difference among groups (*N*=40 for each group). The vertical bar represents one standard deviation.

signal was widely spread in the embryos body from head to tail including some part of the yolk with differentiating or migrating cells (supplementary material Fig. S1). Autofluorescence in the yolk can be distinguished from GFP signal by comparison with the control group without injection. Based on the result, the antisense MO injection was specific for *atp2b1a* as co-injection of capped mRNAs with antisense MO completely blocked the GFP signal in 1–2 dpf embryos (supplementary material Fig. S1). Hence, the phenotype of MO-injected embryos is not due to MO cytotoxicity.

Otolith size and phenotypes

Comparison of the otolith size in wild-type fish and *atp2b1a* morphants showed that starting from 2 dpf, the otoliths are significantly smaller in morphants than in wild-type fish at the same point in development. Higher doses of antisense MO (12 ng) against *atp2b1a* resulted in smaller otoliths (Fig. 5). Phenotype analysis of otoliths among morphants injected with 6 ng *atp2b1a* antisense MO showed differences in formation and localization (Table 1). Otolith formation occurred in most *atp2b1a* morphants but otoliths were mis-localized and in some cases odd numbered otoliths were formed, such as the fish with three otoliths shown in Fig. 4F. The absence of one or both otoliths and fused otoliths on one or both sides was also observed in individual *atp2b1a* morphants.

Semicircular canal phenotypes

The phenotype of the semicircular canal was analyzed using the same group of *atp2b1a* morphants (Table 1). The *atp2b1a* morphants showed abnormal semicircular canal formation, with disrupted or even absent semicircular canal outgrowth (Fig. 4D–F). The defects of otolith formation and semicircular outgrowth always appeared simultaneously in individuals.

Staining of hair cells in the lateral line and inner ear

At 5 dpf, *atp2b1a* morphants had a mean of 4.8 (±1.9; *N*=20; Fig. 6A,B) hair cells in the first neuromast of the posterior lateral line (Metcalfe et al., 1985), whereas wild-type zebrafish had a mean of 8.7 (±1.9; *N*=16; Fig. 6C,E) hair cells. Hair cells in the neuromast of *atp2b1a* morphants were significantly less numerous than in wild-type zebrafish ($P<0.001$, Mann–Whitney rank sum test). The vital mitochondrial dye DASPEI is used for convenient visualization of different epidermal cells in both *in vivo* and *in vitro* studies (Hiroi et al., 1999). In some cases, neuromast hair cells were totally absent in *atp2b1a* morphants although the epidermal ionocytes were stained normally (Fig. 6D).

The tether cells were revealed by HCS-1 antibody in both wild-type larvae and *atp2b1a* morphants at 35 hpf (Fig. 7A–H). At 35 hpf, the wild-type larvae had a pair of two adjoining tether cells, two in the anterior and two in the posterior placode (Fig. 7A,B). The morphants usually had a pair of these adjoining tether cells but some defects were observed. As shown in Fig. 7C,D, there was only one tether cell in the posterior area of the distorted placode. Loss of tether cells in the anterior placode (Fig. 7E,F) and the development of tether cells in the wrong location was also observed. A pair of tether cells appeared in the inside of the placode rather than their correct location at the anterior end (Fig. 7G,H). The inner ear of *atp2b1a* morphants was smaller with the anterior and posterior macula being much closer to each other than in the wild-type fish (Fig. 7K,L). Furthermore, *atp2b1a* morphants had significantly fewer hair cells in the sensory macula and cristae ($P<0.001$, Mann–Whitney rank sum test; Table 2). As shown in Fig. 7J, there was only one hair cell in the posterior crista and two hair cells in the lateral crista of *atp2b1* morphants whereas normal fish (Fig. 7I) had approximately five to seven hair cells in the lateral crista at the same stage of development.

Whole-body calcium influx and contents

Calcium influx and content increased abruptly beginning at 2 dpf in both wild-type zebrafish and *atp2b1a* morphants, indicating increased need for calcium. However, whole-body calcium influx and content measurements were similar in *atp2b1a* morphants and wild-type zebrafish at 2, 4 and 6 dpf (supplementary material Fig. S2). The analysis indicated that calcium absorption was still normal in zebrafish *atp2b1a* morphants. Calcium ions were presumably absorbed through the epithelial ionocytes (Pan et al., 2005). DASPEI staining revealed the normal development and function of epithelial ionocytes on the skin of the *atp2b1a* morphants larvae until at least 6 dpf (Fig. 6D). These results imply that Atp2b1a was not obligatory for the whole-body calcium absorption but might have specific functions in inner ear calcium transport.

DISCUSSION

Functions of Atp2b1a in inner ear morphogenesis

Hair bundles are responsible for mechanotransduction in the hair cells in the inner ear. The development of hair bundles involves multiple interactions with surrounding proteins and morphological

Table 1. Otolith phenotypes and semicircular canal phenotypes in zebrafish *atp2b1a* morphants (4 dpf) injected with 6 ng of *atp2b1a* antisense morpholino

Otolith phenotype			Semicircular canal phenotype		
Normal	Both otoliths lost on one side	One otolith lost or two otoliths fused on one side	Normal	Absence of semicircular canal	Little or disrupted outgrowth
22%	3%	75%	34.3%	1.4%	64.3%

N=120. The control fish received mismatched morpholino injections (6 ng); all showed normal phenotypes (*N*>300).

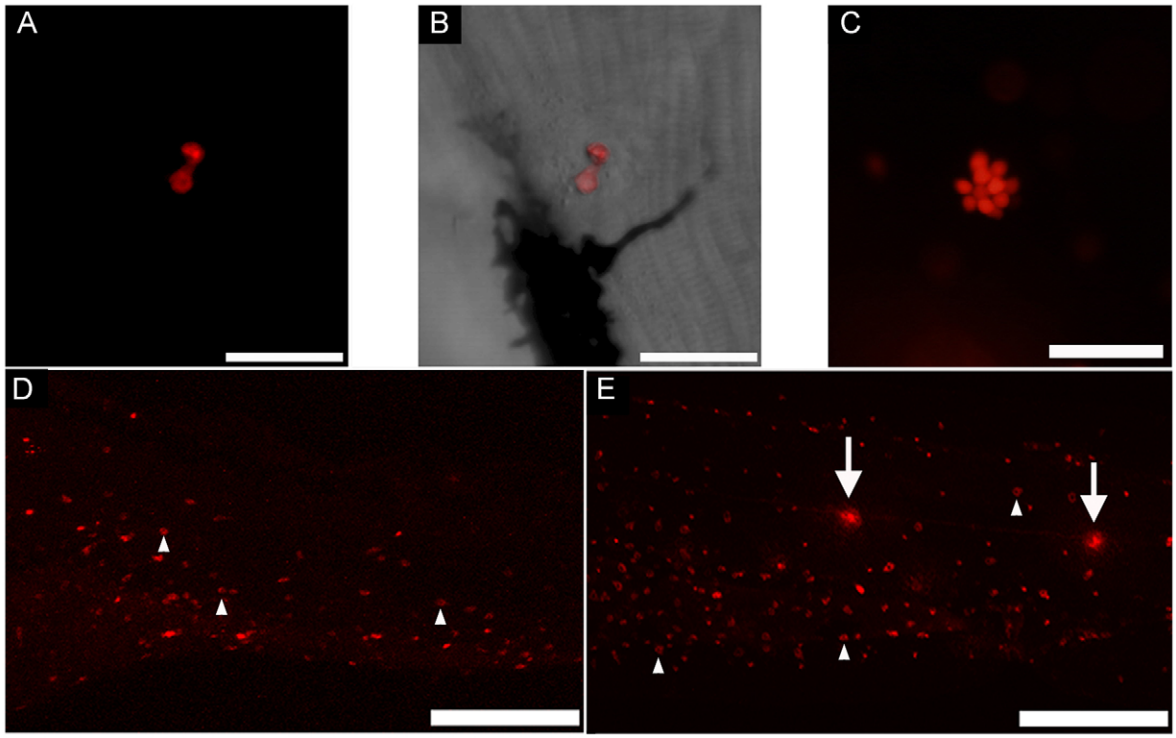

Fig. 6. Staining of hair cells in the neuromast. (A,B) DASPEI staining of zebrafish *atp2b1a* morphants (5 dpf) reveal only two hair cells and less dye absorption in the hair cells of the neuromasts. (C) Wild-type larvae have 10 hair cells in the neuromast and normal uptake of the dye. Arrows indicate the third and fourth neuromasts on the trunk lateral lines. (D,E) The same area of a morphant and normal fish, respectively. Both show normal DASPEI staining of the epithelial ionocytes, indicated by the arrowheads. Scale bar, 25 μm (A–C); 200 μm (D,E).

components (Bryant et al., 2002). The Ca^{2+} that enters through transduction channels is essential to hair bundle function. However, elevated Ca^{2+} concentration is toxic to the cells and regulation of Ca^{2+} concentration is critical. Plasma membrane Ca^{2+} ATPase (PMCA) has been shown to be localized in the hair bundle of bullfrog hair cells (Yamoah et al., 1998) and to be responsible for Ca^{2+} extrusion from hair cell stereocilia, which control intracellular Ca^{2+} concentration (Yamoah et al., 1998). In the present study, inhibition of *atp2b1a* expression reduced the number of hair cells in the inner ear and in the neuromast along the lateral line of zebrafish. Loss of plasma membrane Ca^{2+} ATPase in the hair bundle of *atp2b1a* morphants may cause the breakdown of cellular calcium homeostasis, triggering the death of the hair cells. However, further studies are needed to justify these speculations.

Early regulators of inner ear development have been extensively studied in zebrafish; among these regulators are Fgf, Dlx5, Hmx, Fox and Pax genes (Noramly and Grainger, 2002; Mackereth et al., 2005). Evidently, *atp2b1a* was not required for early otic induction but was essential for semicircular canal morphogenesis. In the present study, we demonstrated that *atp2b1a* knockdown reduced the number of hair cells in the sensory cristae. The sensory cristae and semicircular canals develop during the same period of 42–72 hpf. Mechanisms of semicircular canal formation are conserved among vertebrates (Haddon and Lewis, 1996). As demonstrated in chickens by Chang et al. (Chang et al., 2004), sensory cristae are responsible for the formation of their non-sensory components, the semicircular canals. Abnormal sensory cristae, with few hair cells, may lead to defective development of the semicircular canals by reducing the secretion of hyaluronan-rich matrix (Haddon and Lewis, 1991). Moreover, neuronal calcium sensor (NCS) proteins are also involved in semicircular canal formation in zebrafish (Blasiole et al., 2005). Although the function of NCS in regulating semicircular canal formation is still unclear, NCS may play a role in maintaining endolymphatic calcium homeostasis through interactions with ion transporters such as Atp2b1a (Blasiole et al., 2005). The breakdown of cellular calcium homeostasis by *atp2b1a* knockdown may cause the dysfunction of NCS, influencing the development of the semicircular canal.

Otolith formation, localization and growth

Several otolith phenotypes were observed in *atp2b1a* morphants. The absence of one or both otoliths (Table 1) indicated the failure of initial otolith seeding and subsequent biomineralization with $CaCO_3$. Glycogen is one of the factors responsible for the early formation of

Table 2. The number of hair cells in the sensory macula and cristae of wild-type zebrafish and *atp2b1a* morphants at 4 dpf

	Anterior macula	Anterior cristae	Posterior cristae	Lateral cristae
Wild-type fish (*N*=7)	32.1±7.5	6.7±1.5	7.3±1.0	7.4±1.7
atp2b1a morphant (*N*=13)	13.8±3.2	2.8±1.3	3.0±1.2	1.8±1.3

Values are mean ± standard deviation; *N*=sample size. After HCS-1 antibody and FITC-phalloidin staining, the hair cells were counted from the dorsal view under the confocal microscope. The hair cells in the posterior macula appear overlapped from the dorsal view and so were not counted. Statistical analysis suggests significantly fewer hair cells in *atp2b1a* morphants than in the wild-type zebrafish for each corresponding tissue.

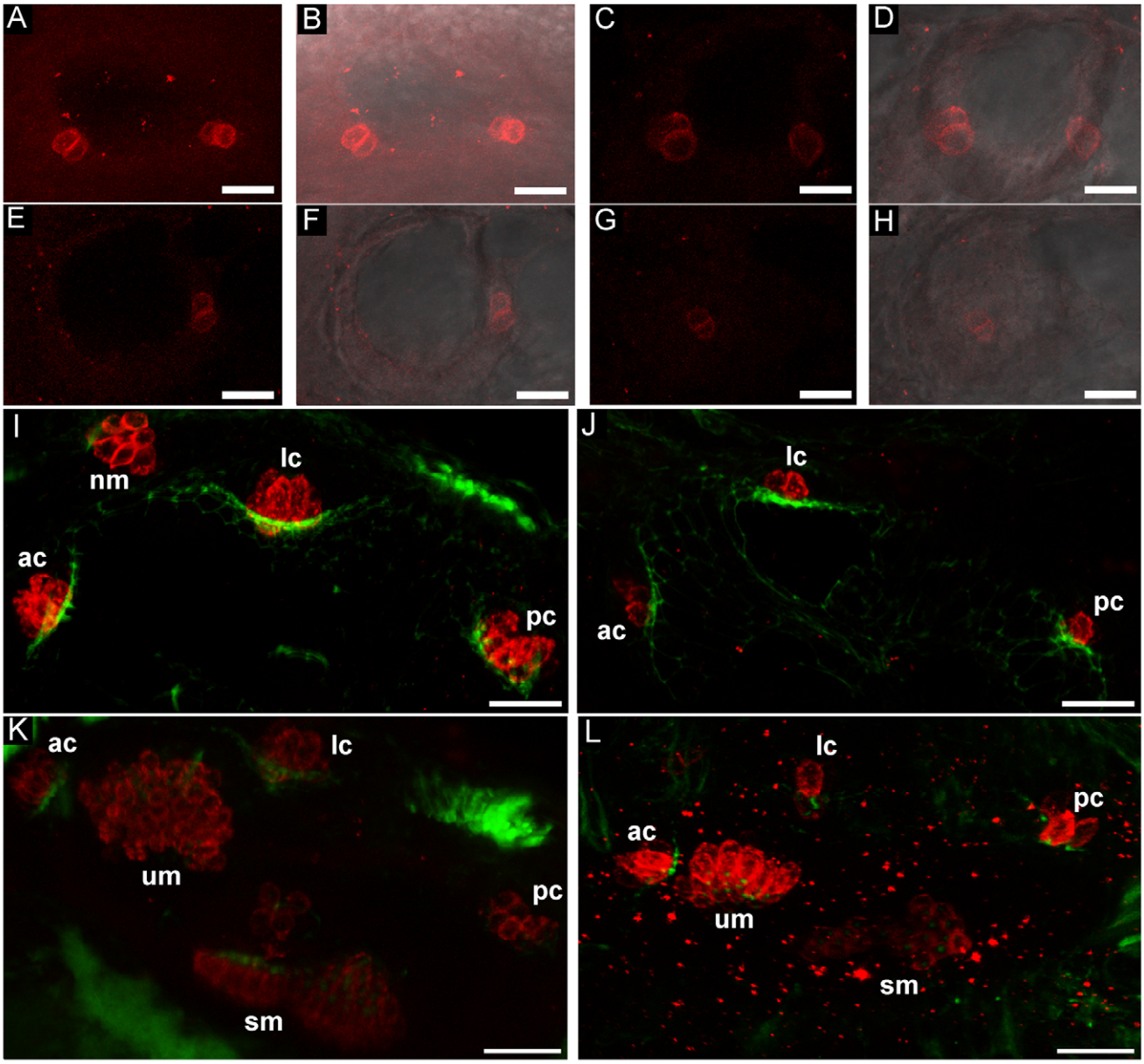

Fig. 7. Staining of hair cells in the inner ear. (A–H) The tether cells are revealed by HCS-1 antibody staining in wild-type larvae (A,B) and *atp2b1a* morphants (C–H) at 35 hpf. Morphants may lose the tether cells or the tether cells develop in the wrong location. E,F and G,H show the tether cells in the posterior region and middle area, respectively. (I–L) FITC-phalloidin (green) and HCS-1 antibody (red) staining of the hair cells in zebrafish inner ear at 4 dpf. There are fewer hair cells in the macula and crista in *atp2b1a* morphants (J,L) than in the wild-type (I,K). ac, lc, pc, anterior, lateral and posterior cristae; nm, neuromast; sm, saccule macula; um, utricular macula. Scale bars, 20 μm for all panels.

the otolith by allowing the insertion of otolith precursors (Pisam et al., 2002). After the initial otolith seeding process at 18 to 24 hpf (Riley et al., 1997), precursors of sagittae and lapilli normally lie in posterior and anterior positions, respectively. Failure of glycogen secretion or accretion of otolith precursor particles may explain the absence of one or both otoliths in *atp2b1a* morphants, as shown in Fig. 4A,B. As observed in many *atp2b1a* morphants, fused otoliths were most probably formed after the seeding process due to the misplacement of the sagittae and lapilli precursors. Fewer cells and development of tether cells in the wrong location may prevent the hair cells from fixing the otolith precursors in the proper position in the macula. In agreement with previous knockdown of the zebrafish chaperone protein GP96 (also known as Hsp90b1), only one otolith was formed in the *atp2b1a* larvae since precursor particles did not adhere to the kinocilia of the tether cells (Sumanas et al., 2003). In addition, zebrafish $Na,^{+}K^{+}$-ATPase α1a.1 knockdown has been shown not to damage the tether cells but completely blocked otolith formation (Blasiole et al., 2006). $Na,^{+}K^{+}$-ATPase coordinates with other ion exchangers and transporters, including Atp2b1a, to maintain endolymph homeostasis (Mugiya and Yoshida, 1995; Shiao et al., 2005). Therefore, knockdown of zebrafish Na^{+},K^{+}-ATPase α1a.1 may result in the failure of the ion exchange system, including that for Ca^{2+} and HCO_3^{-}, and impair otolith formation.

Calcium ion transportation in the inner ear

Otolith accretion by larval zebrafish was affected by *atp2b1a* knockdown, possibly by affecting endolymph composition. However, our data showed equal amounts of whole-body calcium

in wild-type fish and *atp2b1a* morphants during the very early stages. This can be attributed to maternal effects, based on the previous study of Peng et al. (Peng et al., 2003). The control and the morphants group showed a linear increase in calcium levels between days 2 and 6. This implies normal acquisition of calcium through the ionocytes (Pan et al., 2005), as supported by DASPEI staining of ionocytes and normal calcium influx among morphants. However, the inner ear manifested abnormal phenotypes during the early stages when calcium balance in the embryo was still normal. Hence zebrafish Atp2b1a appears to be an active calcium transporter that is essential for normal development and function in the inner ear of larval zebrafish, but is not required for whole-body Ca^{+} uptake from ambient waters.

The confirmation of an Atp2b1a isoform in zebrafish inner ear strengthens and supports previous findings by Mugiya and Yoshida (Mugiya and Yoshida, 1995) in trout. They concluded that an active ATP-dependent calcium pump was involved in the cytosolic calcium extrusion across the sacculus cell apical membrane facing the otolith. Their observations were based on calcium deposition into the otolith under different chemical inhibitors or blockers of calcium transporters/channels. Although we conducted immunohistochemical staining in this study, the antibodies against human ATP2B, i.e. 5F10 (Sigma) (Yamoah et al., 1998) and others (Stauffer et al., 1995) failed to show specific binding to zebrafish Atp2b1a in both larval and adult tissues (the results are not shown). Therefore, the distribution of Atp2b1a in the related cells of the zebrafish inner ear needs further investigation. However, since otolith growth did not completely cease without Atp2b1a, the possible involvement of other Atp2b isoforms or the passive diffusion of calcium into the endolymph cannot be completely excluded. Moreover, abnormal inner ears in *atp2b1a* morphants may cause the tight junctions to be leaky, providing enough local calcium availability for reduced otolith growth.

The presence of other zebrafish Atp2b isoforms needs further study in zebrafish inner ear development. To complete the active transepithelial calcium transport model in the inner ear of zebrafish, further study is required to identify the calcium transporters/channels at the basolateral membrane of the otolith chamber, either from molecular, biochemical or cellular methods.

This study demonstrates *atp2b1a* expression and its major role in otolith formation and semicircular canal development of a teleost fish. Based on our results, zebrafish Atp2b1a has a basic role in the active plasma membrane calcium pump which may influence sensory organ development *via* control of calcium concentration homeostasis in either single hair cells or the whole otic chamber.

We are very grateful to C. I. Wang and C. Y. Lin for their assistance with the experiment and appreciate the valuable review by A. Richardson and D. Cairns. The present work was financially supported by the Thematic Project of the Academia Sinica and the National Science Council of Taiwan. Contract No. AS-95-TP-B05.

REFERENCES

Blasiole, B., Kabbani, N., Boehmler, W., Thisse, B., Thisse, C., Canfield, V. and Levenson, R. (2005). Neuronal calcium sensor-1 gene ncs-1a is essential for semicircular canal formation in zebrafish inner ear. *J. Neurobiol.* **64**, 285-297.

Blasiole, B., Canfield, V., Vollrath, M., Huss, D., Mohideen, M., Dickman, D., Cheng, K., Fekete, D. and Levenson, R. (2006). Separate Na,K-ATPase genes are required for otolith formation and semicircular canal development in zebrafish. *Dev. Biol.* **294**, 148-160.

Borelli, G., Mayer-Gostan, N., de Pontual, H., Boeuf, G. and Payan, P. (2001). Biochemical relationships between endolymph and otolith matrix in the trout (*Oncorhynchus mykiss*) and turbot (*Psetta maxima*). *Calcif. Tissue. Int.* **69**, 356-364.

Bryant, J., Goodyear, R. J. and Richardson, G. P. (2002). Sensory organ development in the inner ear: molecular and cellular mechanisms. *Br. Med. Bull.* **63**, 39-57.

Chang, W., Brigande, J. V., Fekete, D. M. and Wu, D. K. (2004). The development of semicircular canal in the inner ear: role of FGFs in sensory cristae. *Development* **131**, 4201-4211.

Chen, Y. Y., Lu, F. I. and Hwang, P. P. (2003). Comparisons of calcium regulation in fish larvae. *J. Exp. Zool.* **295A,** 127-135.

Campana, S. E. and Neilson, J. D. (1985). Microstructure of fish otoliths. *Can. J. Fish. Aquat. Sci.* **42**, 1014-1032.

Finley, J. E., Xia, B. and Corwin, J. T. (1997). Monoclonal antibodies raised as markers for supporting cells and hair cells. *Assoc. Res. Otolaryngol. Abstr.* **20**, 134.

Furuta, H., Luo, L., Hepler, K. and Ryan, A. F. (1998). Evidence for differential regulation of calcium by outer versus inner hair cells: plasma membrane Ca^{2+}-ATPase gene expression. *Hear. Res.* **123**, 10-26.

Haddon, C. M. and Lewis, J. H. (1991). Hyaluronan as a propellant for epithelial movement: the development of the semicircular canals in the inner ear of *Xenopus*. *Development* **112**, 541-550.

Haddon, C. M. and Lewis, J. H. (1996). Early ear development in the embryo of the zebrafish, *Danio rerio*. *J. Comp. Neurol.* **365**, 113-128.

Harris, J. A., Cheng, A. G., Cunningham, L. L., MacDonald, G., Raible, D. W. and Rubel, E. W. (2003). Neomycin-induced hair cell death and rapid regeneration in the lateral line of zebrafish (*Danio rerio*). *J. Assoc. Res. Otolaryngol.* **4**, 219-234.

Hiroi, J., Kaneko, T. and Tanaka, M. (1999). In vivo sequential changes in chloride cell morphology in the yolk-sac membrane of mozambique tilapia (*Oreochromis mossambicus*) embryos and larvae during seawater adaptation. *J. Exp. Biol.* **202**, 3485-3495.

Hwang, P. P. and Lee, T. H. (2007). New insights into fish ion regulation and mitochondrion-rich cells. *Comp. Biochem. Physiol.* **148A**, 479-497.

Ibsch, M., Anken, R., Beier, M. and Rahmann, H. (2004). Endolymphatic calcium supply for fish otolith growth takes place via the proximal portion of the otocyst. *Cell. Tissue. Res.* **317**, 333-336.

Kozel, P. J., Friedmans, R. A., Erway, L. C., Yamoah, E. N., Liu, L. H., Riddle, T., Duffy, J. J., Doetschman, T., Miller, M. L., Cardell, E. L. et al. (1998). Balance and hearing deficits in mice with a null mutation in the gene encoding plasma membrane Ca^{2+}-ATPase isoform 2. *J. Biol. Chem.* **273**, 18693-18696.

Kumar, S., Tamura, K. and Nei, M. (2004). MEGA3: integrated software for molecular evolutionary genetics analysis and sequence alignment. *Brief. Bioinformatics* **5**, 150-163.

Liao, B. K., Deng, A. N., Chen, S. C., Chou, M. Y. and Hwang, P. P. (2007). Expression and water calcium dependence of calcium transporter isoforms in zebrafish gill mitochondrion-rich cells. *BMC Genomics* **8**, 354.

Mackereth, M. D., Kwak, S. J., Fritz, A. and Riley, B. B. (2005). Zebrafish pax8 is required for otic placode induction and plays a redundant role with pax2 genes in the maintenance of the otic placode. *Development* **132**, 371-382.

Metcalfe, W., Kimmel, C. B. and Schabtach, E. (1985). Anatomy of the posterior lateral line system in young larvae of the zebrafish. *J. Comp. Neurol.* **233**, 377-389.

Mugiya, Y. and Yoshida, M. (1995). Effects of calcium antagonist and other metabolic modulators on *in vitro* calcium deposition on otoliths in the rainbow trout *Oncorhynchus mykiss*. *Fisheries Sci.* **61**, 1026-1030.

Noramly, S. and Grainger, R. M. (2002). Determination of the embryonic inner ear. *J. Neurobiol.* **53**, 100-128.

Pan, T. C., Liao, B. K., Huang, C. J., Lin, L. Y. and Hwang, P. P. (2005). Epithelial Ca^{2+} channel expression and Ca^{2+} uptake in developing zebrafish. *Am. J. Physiol. Regul. Integr. Comp. Physiol.* **289**, R1202-R1211.

Payan, P., Borelli, G., Priouzeau, F., de Pontual, H., Boeuf, G. and Mayer-Gostan, N. (2002). Otolith growth in trout *Oncorynchus mykiss*: supply of Ca^{2+} and Sr^{2+} to the saccular endolymph. *J. Exp. Biol.* **205**, 2687-2695.

Peng, J. B., Brown, E. M. and Hediger, M. A. (2003). Apical entry channels in calcium-transporting epithelia. *News Physiol. Sci.* **18**, 158-163.

Pisam, M., Jammet, C. and Laurent, D. (2002). First steps of otolith formation of the zebrafish: role of glycogen? *Cell. Tissue. Res.* **310**, 163-168.

Popper, A. N. and Fay, R. R. (1997). Evolution of the ear and hearing: issues and questions. *Brain Behav. Evol.* **50**, 13-221.

Popper, A. N. and Lu, Z. (2000). Structure function relationship in fish otolith organs. *Fish. Res.* **46**, 15-25.

Riley, B. B., Zhu, C., Janetopoulos, C. and Aufderhaide, K. J. (1997). A critical period of ear development controlled by distinct populations of ciliated cells in the zebrafish. *Dev. Biol.* **191**, 191-201.

Romanek, C. S. and Gauldie, R. W. (1996). A predictive model of otolith growth in fish based on the chemistry of the endolypmh. *Biochem. Physiol.* **114A,** 71-79.

Sasagawa, T. and Mugiya, Y. (1996). Biochemical properties of water-soluble otolith proteins and the immunobiochemical detection of the proteins in serum and various tissues in the tilapia, *Oreochromis niloticus*. *Fisheries Sci.* **62**, 970-976.

Shiao, J. C., Lin, L. Y., Horng, J. L., Hwang, P. P. and Kaneko, T. (2005). How can teleostean inner ear hair cells maintain the proper association with the accreting otolith? *J. Comp. Neurol.* **488**, 331-341.

Shull, G. E. (2000). Gene knockout studies of Ca^{2+}-transporting ATPases. *Eur. J. Biochem.* **267**, 5284-5290.

Stauffer, T. P., Guerini, D. and Carafoli, E. (1995). Tissue distribution of the four gene products of the plasma membrane Ca^{2+} pump. *J. Biol. Chem.* **270**, 12184-12190.

Sumanas, S., Larson, J. D. and Bever, M. M. (2003). Zebrafish chaperone protein GP96 is required for otolith formation during ear development. *Dev. Biol.* **261**, 443-455.

Whitfield, T. T., Riley, B. B., Chiang, M. Y. and Phillips, B. (2002). Development of the zebrafish inner ear. *Dev. Dyn.* **223**, 427-458.

Yamoah, E. N., Lumpkin, E. A., Dumont, R. A., Smith, P. J., Hudspeth, A. J. and Gillespie, P. G. (1998). Plasma membrane Ca^{2+}-ATPase extrudes Ca^{2+} from hair cell stereocilia. *J. Neurosci.* **18**, 610-624.

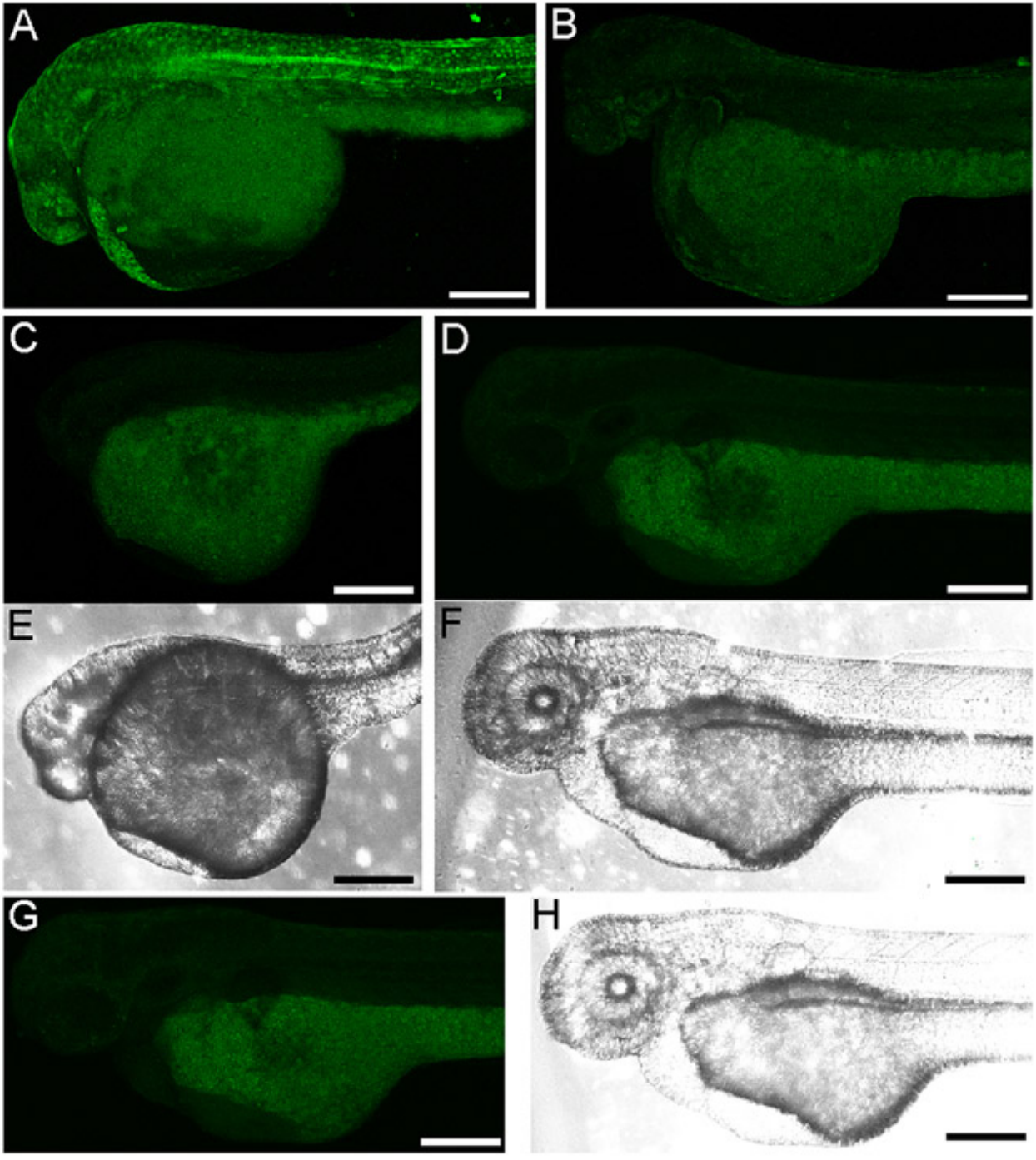
A
B
C
D
E
F
G
H

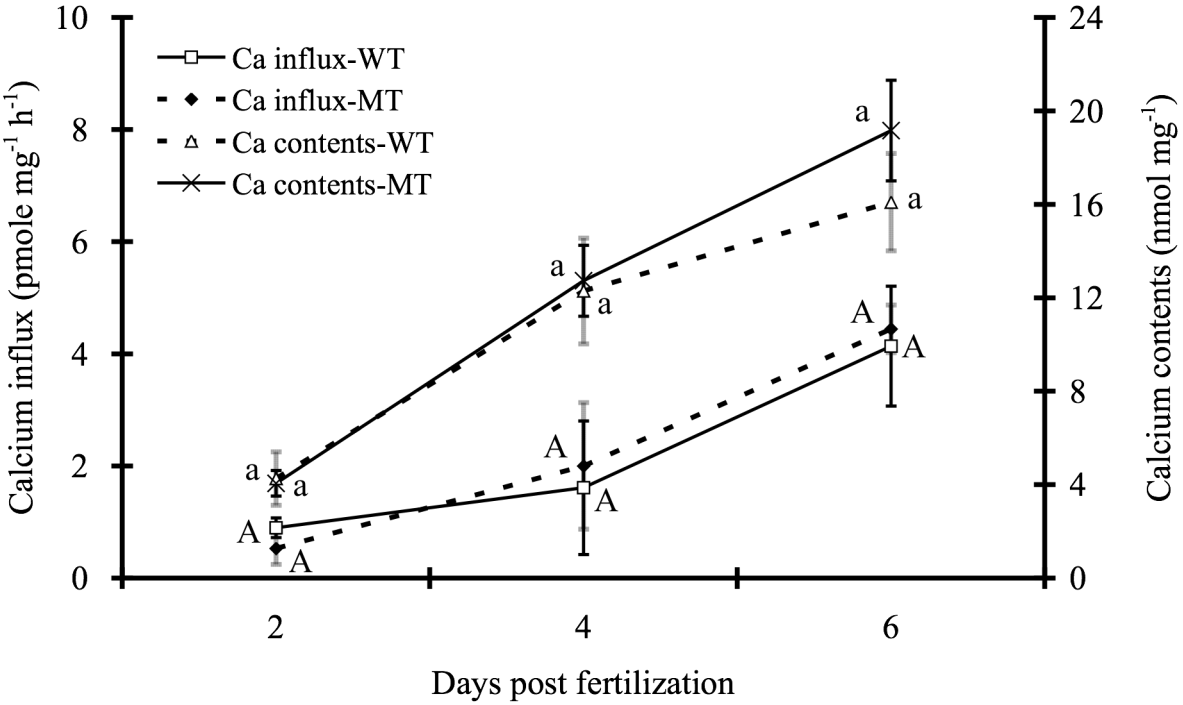
Ca influx-WT
Ca influx-MT
Ca contents-WT
Ca contents-MT
Calcium influx (pmole mg-1 h-1)
Calcium contents (nmol mg-1)
Days post fertilization
0
2
4
6
8
10
12
16
20
24
a
A